Macromolecules **1992,** *25,* 6377–6380

Appearance of a Moving Droplet Phase and Unusual Networklike or Spongelike Patterns in a Phase-Separating Polymer Solution with a Double-Well-Shaped Phase Diagram

Hajime Tanaka

Department of Applied Physics and Applied Mechanics, Institute of Industrial Science, University of Tokyo, Minato-ku, Tokyo 106, Japan

Received June 18, 1992
Revised Manuscript Received August 14, 1992

Generally, the dynamics and morphology of phase separation are strongly dependent on the quench conditions. From this standpoint, phase-separation phenomena are divided into nucleation growth (NG) and spinodal decomposition (SD) in the mean-field picture.[1-3] In the unstable region where SD occurs, decomposition generally proceeds faster with an increase in the quench depth since the thermodynamic driving force for phase separation becomes stronger. So far there has been no exception to the above quench depth dependence of phase-separation speed.[1,2] It has also been believed that the phase-separated pattern coarsens with time to reduce interfacial energy and that the system finally separates into two macroscopic phases, provided there is no coupling between phase separation and other ordering processes such as crystallization.[4]

In this paper, we present the first exception to the above general law of phase separation. We demonstrate new phenomena which cannot be explained by the above conventional scheme of phase separation. Previously we reported an anomalous phase separation,[5] although in that case the mechanism was not clear. Here we find that a double-well-shaped phase diagram (DWSPD) is responsible for an anomalous phase with moving droplets where there is no coarsening with time. We also find interesting and unusual phase-separated morphologies, with networklike and spongelike structures, probably for the first time. The mechanisms of these unusual phenomena will be discussed.

Samples used were mixtures of poly(vinyl methyl ether) (PVME) and water. The weight-average and number-average molecular weights of PVME were 108 200 and 48 300, respectively. The distribution of the degree of polymerization (N) was approximated by the function $P(N) \sim (1/N) \exp[-((\log N - 3.24)/0.37)^2]$. The mixture has a lower critical solution temperature (LCST). The sample sandwiched between two cover glasses (a typical thickness of about several microns) was set horizontally on the temperature-controlled hot stage (Linkam TH-600RMS). The heating rate used in the experiment was 1.5 °C/s. The phase-separated pattern was observed by phase-contrast microscopy.

The phase diagram of the system is shown in Figure 1. The solid curve represents a cloud-point curve. The striking characteristic of this phase diagram is its double-well shape.[6] This unusual shape is probably responsible for the interesting phenomena described below. Here we define T_t as the top temperature and T_{b1} and T_{b2} as the two bottom temperatures on the bimodal curve. In the regions numbered as V and VI (below T_t), the usual phase separation occurs with coarsening. In these regions the coarsening rate increases with an increase in the quench depth as usual. In the shaded region numbered I, on the other hand, an anomalous phase separation occurs (see Figure 2). The anomaly is as follows. Small droplets (approximately micron size) are formed immediately after the temperature jump above T_t, and they move around vigorously by Brownian motion without coalescing. There is no coarsening at all, although the droplet density is high enough to cause frequent collisions. This state was checked to be stable at least for 2 days and seems to be stable forever. The morphological transition between the usual SD and the unusual local phase separation coincides exactly with a dynamic transition in the motional state of droplets. The number density of droplets increases almost monotonically with an increase in the polymer concentration ϕ (see Figure 2).

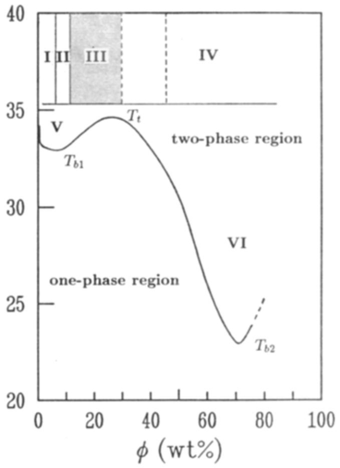

Figure 1. Phase diagram for PVME and water. ϕ is the polymer concentration. I corresponds to a phase with moving droplets (MDP), III to a phase with a networklike pattern (NP), II to the transition region where MDP and NP coexist together, and IV to a phase with a spongelike pattern. The boundary between III and IV is diffuse between the two dashed lines. In the regions V and VI, the usual phase-separation behavior is observed.

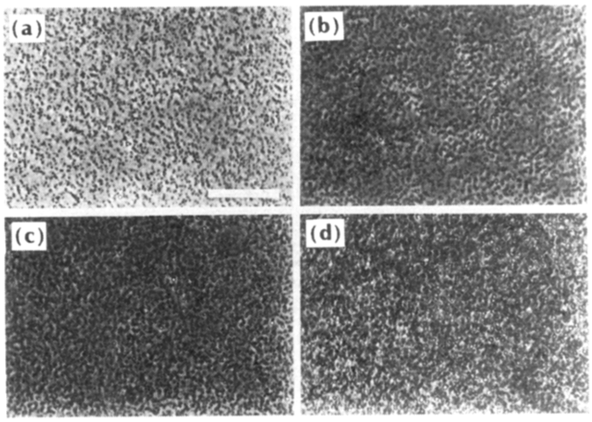

Figure 2. Photographs of MDP observed in region I for different ϕ: (a) 2 wt % at 37.3 °C, (b) 3 wt % at 37.5 °C, (c) 5 wt % at 37.6 °C, and (d) 7 wt % PVME at 37.6 °C. The bar corresponds to 40 μm. In these phases, there is no coarsening with time.

The new state seems to be stable, so it should be regarded as a *phase*, which we call the moving droplet phase (MDP). This unusual phenomenon occurs only when the system is quickly heated above T_t. The phase diagram tells us that above T_t the system separates into a very dilute and a very dense polymer phase. This phase-separation process begins with droplet formation, and the droplets grow to a certain size. Then, during the temperature jump, the droplet starts to shrink quickly by discharging water just after the temperature exceeds T_t. This process is probably responsible for the formation of a small, dense droplet with a final equilibrium composition, which has vigorous Brownian motion. If we lower the temperature of MDP

0024-9297/92/2225-6377$03.00/0

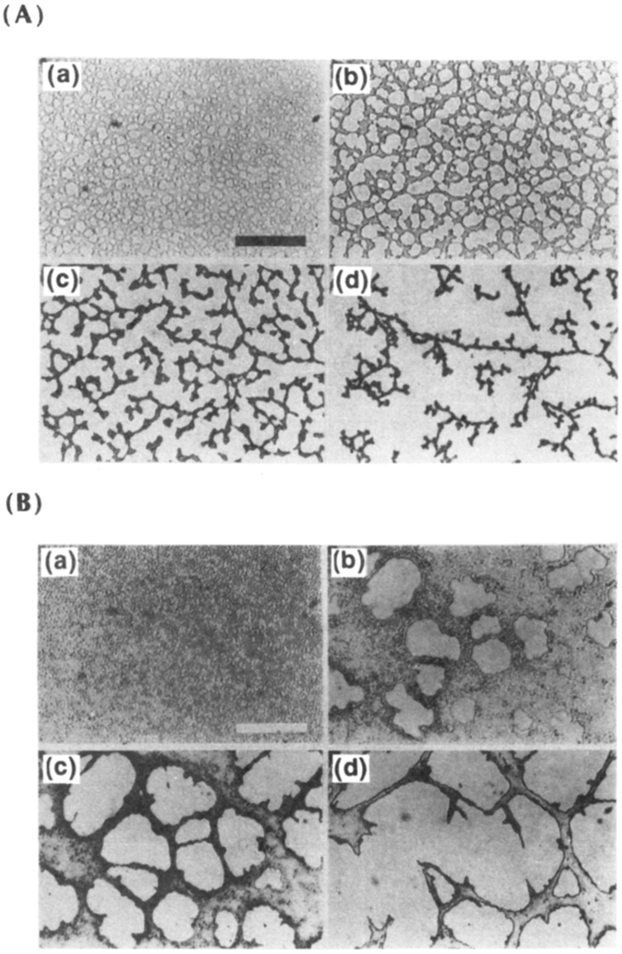

Figure 3. (A) Evolution of the NP observed in region II ($\phi = 7$ wt %, $T = 37.3$ °C) (a) 1 s, (b) 1.4 s, (c) 3 s, and (d) 30 s after the temperature jump. The bar corresponds to 200 μm. In these photographs moving droplets are not observed because of the lack of a dynamic range. (B) Evolution of the NP observed in region III ($\phi = 10$ wt %, $T = 37.4$ °C) (a) 3 s, (b) 4 s, (c) 6 s, and (d) 60 s after the temperature jump. The bar corresponds to 200 μm.

just below T_t, coalescence starts to occur between droplets and a coarsening process accompanies the usual phase separation. Thus, T_t is a *critical* temperature.

In region II (Figure 1), the MDP coexists with the phase (NP) having a unique networklike phase-separated pattern (see Figure 3A). In region III (Figure 1), a networklike phase-separated pattern (NP) is observed (see Figure 3B). These figures show the coarsening process of the NP structure. As the polymer-rich phase discharges water to the surrounding matrix, it shrinks. Thus the coarsening process is mainly governed by shrinkage of the polymer-rich phase as indicated in Figure 3A,B. This coarsening mechanism is unusual and different from that observed during the usual spinodal decomposition near the symmetric composition in an interconnected structure. In region IV (Figure 1) the phase (SP) having a spongelike or Swiss-cheese-like phase-separated structure is observed. Such behavior is observed only above T_t and can be explained by the DWSPD.

The reason why the system has a DWSPD is not clear at the present stage. There are two possibilities accounting for the phenomenon: (1) the effects of hydrogen bonding and hydrophobic interaction[7-10] and (2) a polydispersity effect. These effects may cause the strong dependence of the interaction parameter on the composition, which likely leads to a DWSPD.[6] A weak dependence of the phase-separation temperature on molecular weight[7,9] seems to support the former possibility. The composition ϕ_t, which gives the phase-separation temperature T_t, may be optimum for the interaction between the polymer and water. To clarify the mechanism, we are now planning to perform experiments using fractionated (monodisperse) PVME.

First we consider the stabilization mechanism of the MDP. In the MDP, the Brownian coagulation mechanism[1,2,11-13] does not work, although droplets move vigorously enough by Brownian motion to cause frequent collisions. For particle stabilization, some repulsive interaction is necessary for thermal energy to overcome the London–van der Waals interaction. The reduction of interfacial energy is one possibility, but the formation of a micellelike structure is hard to expect in a binary polymer/water mixture. Furthermore, in this system there is no electrostatic repulsion between droplets. Thus the stabilization mechanism may be similar to the so-called "steric stabilization of polymer-adsorbed particle",[14] caused by the excluded-volume and osmotic-pressure effects. The highly organized water[7-10] around the polymer chain in the interfacial region may enhance the excluded-volume effect and strengthen the steric repulsion. The repulsive interaction between droplets may also be caused by the hydrophobic interaction through the highly organized water.[7-10] Both the steric repulsion and the hydrophobic repulsive interaction are likely consistent with the fact that MDP exists only above T_t. Because of a repulsive interaction there probably exists a minimum accessible distance between droplets, δ. This gives the cutoff for the energy of adhesion and modifies the depth of the attractive interaction potential significantly. If the thermal energy or kinetic energy of droplets ($\sim kT$) is greater than their energy of attraction, coalescence is prevented. Viscous interaction[15] is a kinetic factor which also helps to prevent direct contact between droplets.

Because a droplet is composed of mobile molecules, we need to consider fusion dynamics further. The characteristic time of collision and the characteristic viscoelastic relaxation time can be estimated as follows. Brownian motion of a droplet with mass m corresponds roughly to a randomly varying thermal velocity of magnitude $\langle v \rangle \sim (k_B T/m)^{1/2}$ and duration $\tau_r \sim m D_R / k_B T$ (D_R is the diffusion constant of a droplet with radius R). The contact time τ_c should satisfy the relation $r_0/\langle v \rangle < \tau_c < r_0^2/D_R$, where r_0 is the range of the interaction. r_0 is determined by the interface thickness (correlation length) ξ or the distance ($\sim\delta$) at which the interaction potential has a weak minimum and should be in the microscopic length scale.[16] Here we use τ_c with $r_0 \sim \max\,[\xi, \delta]$ as a characteristic time of binary droplet collision. Next, the terminal time τ_t for reptation of a polymer in a dense polymer matrix (characteristic time of interdiffusion) can be roughly estimated as $a^2 N^3 \Phi^{3/2} / D_1$ (a is the length of a unit monomer, N is the degree of polymerization, Φ is the volume fraction of a polymer, and D_1 is the diffusion constant of a monomer).[17] If we assume $N \sim 10^3$, $D_1 \sim 10^{-6}$ cm^2/s, $a \sim 0.4$ nm, $\Phi \sim 1$, $R \sim 1$ μm, $m \sim (4\pi/3)R^3$, and $r_0 \sim 10$ nm, we obtain $\tau_t \sim 1$ s and 10 μs $< \tau_c <$ 0.5 ms. Thus we conclude τ_t is several orders of magnitude longer than τ_c. Even though the distribution of N due to the polydispersity is taken into account, τ_t is still longer than τ_c almost for the whole range of N. Furthermore, τ_t would be even much larger if there is an attractive interaction or association between polymers above the LCST, as expected from the hydrophobic interaction and hydrogen bonding. A droplet likely behaves as an *elastic body* on the collision time scale. If there is strong association between polymers, the elastic energy may overcome the interfacial energy and prevent coalescence even when droplets do not move vigorously. The elastic behavior of the polymer-rich phase above T_t is evident from the coarsening process of NP.

Here we briefly consider the other coarsening mechanism, namely, the evaporation–condensation mechanism.[1,2,16,18,19] In the MDP a steady diffusion flow necessary for the evaporation–condensation mechanism is prevented by droplet Brownian motion which is much faster than the characteristic speed of diffusion. In other words, the concentration gradient coming from different droplet sizes is blurred by the vigorous droplet motion. These considerations on the two coarsening mechanisms, namely, the Brownian coagulation and evaporation–condensation mechanisms, lead us to the conclusion that the MDP is probably a stable, heterogeneous phase.

If we lower the temperature of the MDP below T_t, droplets start to coalesce with each other. This can be explained as follows. Below T_t a polymer-rich droplet starts to absorb water from the matrix in order to reach the new, final equilibrium concentration. As a result, the mobility of the polymer inside the droplet increases rapidly. At the same time, the elastic energy becomes less important than the interfacial energy. Both these effects make droplet coalescence possible. Further, Brownian motion slows down since the droplet expands by absorbing water, and this also helps coalescence.

Next we discuss the unusual phase-separated morphologies observed in regions II–IV. The boundary composition between I and III likely coincides with the percolation threshold (the phase inversion composition between matrix and droplet) for the left-hand side of the DWSPD (region V), because the phase separation is initiated in region V even under a quick temperature-jump condition (1.5 °C/s in our case). Below this composition a polymer-rich phase appears as small droplets in a water-rich matrix and the droplets shrink by discharging water and densifying above T_t. Above this composition, on the other hand, the water-rich phase initially appears as droplets in a polymer-rich matrix. The matrix shrinks by discharging water and adopting the networklike structure. Eventually it becomes very thin, since the final volume of the polymer-rich phase should be very small in region III. However, in region IV, the final volume fraction of the polymer-rich phase is high enough to form the spongelike phase. The boundary composition between III and IV probably corresponds to the symmetric composition for the DWSPD above T_t. In both regions III and IV, as the polymer-rich matrix shrinks and becomes more concentrated, a tensile force acts along the thin part of the matrix. If the elongated part is not thick enough to support the tension, it splits in two and relaxes to the force-free shape. The elastic energy dominates the coarsening behavior instead of the surface energy, and this causes the unusual patterns. Locally, the networklike pattern has a geometrical characteristic unique to two-dimensional (2D) systems: the angle between branches approximates 120° in many places, reflecting the force-balance condition.

In regions I–III, a polymer-rich phase shrinks drastically just after the temperature jump above T_t and keeps shrinking until the composition reaches its final equilibrium state (very dense polymer). The temporal change in the volume of the polymer-rich phase is readily observed (Figure 3). This indicates that the concentration keeps changing even after the formation of a sharp interface. This behavior apparently violates the conventional assumption[1,2] that after the formation of a sharp interface a system is in a local equilibrium state with an equilibrium phase composition. For the DWSPD there is a large difference in the equilibrium compositions between below and above T_t. This causes the composition inconsistency between the initial and late stages of phase separation: The final equilibrium compositions for the initial stage of phase separation are determined by the DWSPD below T_t, while those for the late stage are determined by the DWSPD above T_t. Thus the behavior observed is probably the relaxation process of the composition inconsistency by diffusion. The relaxation time seems to depend on a characteristic size of the polymer-rich phase. The process appears to be similar to the shrinkage of the gel where the characteristic shrinking time is given by L^2/D (D is the diffusion constant of the gel, L is the characteristic length of the gel). The polymer-rich phase could behave like the gel because of the strong entanglement or association between polymers. Thus, this unusual phenomenon probably comes from the characteristic shape of the DWSPD and also the fact that the system separates into two phases having different viscoelastic properties pertaining to a chainlike macromolecule and a small molecule. We need further theoretical and experimental studies on this problem.

In summary, we have found a moving droplet phase (MDP) in a low polymer concentration region and a networklike or spongelike phase-separated pattern in a high polymer concentration region for a polymer solution exhibiting a LCST-type DWSPD. The double-well shape of the phase diagram is found to be responsible for the unusual phenomena observed in the system. The MDP may be stabilized by dynamic as well as by thermodynamic factors. Specific interactions such as hydrogen bonds and hydrophobic attraction probably cause molecular association which has an important role in the unusual behavior. The chain collapsing transition in the polymer/water mixture may also be related to the existense of MDP. These points are now under investigation.

Recently we have found the existence of a MDP in PNIPA as well,[20] suggesting the generality of such phenomena. In fact, the unusual phenomena found here are likely universal for any polymer solution showing a DWSPD, and possibly even for a polymer solution with a usual phase diagram, provided that the system can be brought deeply and rapidly enough into the unstable region. It should be stressed that the large difference in viscoelastic properties between the two component materials is probably essential for the phenomena.

Acknowledgment. I thank Dr. R. E. Cais for critical reading of the manuscript. This work was partly supported by a Grant-in-Aid from the Ministry of Eduction, Science, and Culture, Japan, by a grant from Kanagawa Academy of Science and Technology, and by a grant from the Iketani Science and Technology Foundation.

References and Notes

(1) Gunton, J. D.; San Miguel, M.; Sahni, P. *Phase Transition and Critical Phenomena*; Domb, C., Lebowitz, J. H., Eds.; Academic: London, 1983.
(2) *Dynamics of Ordering Process in Condensed Matter*; Komura, S., Furukawa, H., Eds.; Plenum: New York, 1987.
(3) Tanaka, H.; Yokokawa, T.; Abe, H.; Hayashi, T.; Nishi, T. *Phys. Rev. Lett.* **1990**, *65*, 3136.
(4) Tanaka, H.; Nishi, T. *Phys. Rev. Lett.* **1985**, *55*, 1102.
(5) Tanaka, H.; Nishi, T. *Jpn. J. Appl. Phys.* **1988**, *27*, L1787.
(6) Koningsveld, R.; Kleintjeus, L. A.; Schoffeleers, H. M. *Pure Appl. Chem.* **1974**, *39*, 1.
(7) Heskins, M.; Guilett, J. E. *J. Macromol. Sci.* **1986**, *A2*, 1441.
(8) Winnik, F. M. *Macromolecules* **1990**, *23*, 233.

(9) Otake, K.; Inomata, H.; Konno, M.; Saito, S. *Macromolecules* **1990**, *23*, 283.
(10) Fujishige, S. *Polym. J.* **1987**, *19*, 297.
(11) Binder, K.; Stauffer, D. *Phys. Rev. Lett.* **1974**, *33*, 1006.
(12) Binder, K.; Stauffer, D. *Adv. Phys.* **1976**, *25*, 343.
(13) Binder, K. *Phys. Rev.* **1977**, *B15*, 4425.
(14) Israerachivili, J. N. *Intermolecular and Surface Forces*; Academic: New York, 1985.
(15) Spielman, L. A. *J. Colloid Interface Sci.* **1970**, *33*, 562.
(16) Siggia, E. D. *Phys. Rev.* **1979**, *A20*, 595.
(17) de Gennes, P.-G. *Scaling Concepts in Polymer Physics*; Cornell University Press: Ithaca, NY, 1979.
(18) Lifshits, I. M.; Slyozov, V. V. *J. Phys. Chem. Solids* **1961**, *19*, 35.
(19) Wagner, C. *Z. Electrochem.* **1961**, *65*, 581.
(20) Tanaka, H., unpublished.

Registry No. H_2O, 7732-18-5.

CORRECTIONS

B. Erman* and J. E. Mark: Stress–Strain Isotherms for Elastomers Cross-Linked in Solution. 2. Interpretation in Terms of the Constrained-Chain Model. Volume 25, Number 7, March 30, 1992, pp 1917–1921.

The analysis of experimental data presented in this paper was based on the model described in a theoretical study (Erman, B.; Monnerie, L. *Macromolecules* **1989**, *22*, 3342) which was found to have errors in several of the equations. The corrected equations in the analysis paper are given by

$$B_x = h(\lambda_x)^2\left[\frac{\kappa_G\lambda_x{}^2}{h(\lambda_x)} - 1\right]/[\lambda_x{}^2 + h(\lambda_x)]^2$$

$$D_x = \lambda_x{}^2 B_x/h(\lambda_x) \tag{5}$$

$$h(\lambda_x) = \kappa_G[1 + (\lambda_x{}^2 - 1)\Phi]$$

and

$$B = h(\lambda)\,\kappa_G(1 - \Phi)(\lambda^2 - 1)/[\lambda^2 + h(\lambda)]^2$$

$$D = \lambda^2 B/h(\lambda) \tag{10}$$

$$\dot{B} \equiv \frac{\partial B}{\partial \lambda^2} = B\left\{(\lambda^2 - 1)^{-1} - 2[\lambda^2 + h(\lambda)]^{-1} + \frac{\kappa_G}{h}\frac{(\lambda^2 - h)\Phi}{[\lambda^2 + h(\lambda)]}\right\}$$

$$\dot{D} \equiv \frac{\partial D}{\partial \lambda^2} = B\left[h(\lambda)^{-1} - \frac{\lambda^2\kappa_G\Phi}{h(\lambda)^2}\right] + \frac{\lambda^2\dot{B}}{h(\lambda)}$$

The effects of these changes on the constants obtained in the analysis are minor [$A = 1.87$ (previously 1.29) and $m = 0.385$ (previously 0.82)] and do not affect any of the conclusions reached in this study.

We thank Dr. Andrzej Kloczkowski of the University of Cincinnati, Department of Chemistry, for pointing out this error to us.